Catalysis Science & Technology

PAPER

View Article Online
View Journal | View Issue

The effect of oxide acidity on HMF etherification†

Jing Luo,[a] Jingye Yu,[a] Raymond J. Gorte,‡*[a] Eyas Mahmoud,[b] Dionisios G. Vlachos[b] and Michael A. Smith[c]

Cite this: *Catal. Sci. Technol.*, 2014, **4**, 3074

Received 1st May 2014, Accepted 31st May 2014

DOI: 10.1039/c4cy00563e

www.rsc.org/catalysis

The liquid-phase (69 bar) reaction of 5-hydroxymethylfurfural (HMF) with 2-propanol for production of furanyl ethers was studied at 413 and 453 K over a series of oxide catalysts, including γ-Al_2O_3, ZrO_2, TiO_2, Al_2O_3/SBA-15, ZrO_2/SBA-15, TiO_2/SBA-15, H-BEA, and Sn-BEA. The acidity of each of the catalysts was first characterized for Brønsted sites using TPD-TGA of 2-propanamine and for Lewis sites using TPD-TGA of 1-propanol. Catalysts with strong Brønsted acidity (H-BEA and Al_2O_3/SBA-15) formed 5-[(1-methylethoxy) methyl]furfural with high selectivities, while materials with Lewis acidity (γ-Al_2O_3, ZrO_2, TiO_2, and Sn-BEA) or weak Brønsted acidity (ZrO_2/SBA-15 and TiO_2/SBA-15) were active for transfer hydrogenation from the alcohol to HMF to produce 2,5-bis(hydroxymethyl)furan, with subsequent reactions to the mono- or di-ethers. Each of the catalysts was stable under the flow-reactor conditions but the selectivities varied with the particular oxide being investigated.

Introduction

The conversion of cellulosic biomass into liquid fuels, or fuel additives, would be attractive if it could be performed economically. While potential processes exist for taking cellulose to C-5 and C-6 sugars, and these can in turn be converted into furfural and 5-hydroxymethylfurfural (HMF), additional processing is required in order to stabilize furfural and HMF because they remain highly functionalized. Since H_2 is expensive to produce and compress and is not economically renewable, processes that avoid its use and minimize its consumption are preferred. One interesting approach for upgrading furfural and HMF that avoid the need for gas-phase H_2 involves reactions with alcohols or aldehydes to produce higher molecular weight products that can be used in diesel fuel, either directly or after minor additions of hydrogen.[1,2] One example where this has been accomplished involves cross-aldol condensation with acetone[3] and hydroxylation.[4]

An alternative approach to aldol condensation involves etherification of HMF with an alcohol. The direct etherification of HMF to form the mono-ether furfural can be catalyzed by Brønsted acids, including H_2SO_4[1] and H-zeolites,[5] as shown in Scheme 1(a). However, the remaining carbonyl functional group in the mono-ether furfurals reduces the stability of the molecule compared to the corresponding alcohols.[1,6] Formation of di-ethers from 2,5-bis(hydroxymethyl)furan (BHMF) has been demonstrated but this requires a two-step process in which the carbonyl group is first reduced.[7] Reductive etherification, in which the carbonyl is hydrogenated and then reacted to form the di-ether, avoids this problem. In a demonstration of this chemistry, Balakrishnan *et al.*[1] reported the one-pot reductive etherification of HMF to form 2,5-bis(alkoxymethyl)furan, shown in Scheme 1(b). This reaction requires H_2 to reduce the carbonyl group, increasing the material and process cost.

Transfer hydrogenation *via* the Meerwein–Ponndorf–Verley (MPV) reaction, shown in Scheme 1(c), provides the opportunity for an interesting variation on reductive etherification, since the alcohol used as the reactant for making the ether can also be used as the hydrogen source. The aldehyde or ketone produced by oxidation of the alcohol would need to be hydrogenated in a separate step, but this subsequent reaction could be carried out in the gas phase and would not require high-pressure H_2.[8] Alternatively, the aldehyde or ketone produced could be used in aldol-condensation of HMF. Some examples where transfer hydrogenation has been used include the following: Petra *et al.*[9] performed transfer hydrogenation over ruthenium(II) for the reduction of acetophenone; Mollica *et al.*[10] reported the reduction of aromatic and aliphatic aldehydes using isopropanol as hydrogen donor and ytterbium triflate as the catalyst; Misra *et al.*[11] applied bimetallic alkoxides of praseodymium and neodymium to carry out the transfer hydrogenation of octanone. Of particular interest, transfer hydrogenation has been shown to be

[a] *Department of Chemical & Biomolecular Engineering, University of Pennsylvania, Philadelphia, PA 19104, USA. E-mail: gorte@seas.upenn.edu, jingluo@seas.upenn.edu; Fax: +1 215 573 2093; Tel: +1 215 898 8351*

[b] *Catalysis Center for Energy Innovation, Department of Chemical & Biomolecular Engineering, University of Delaware, Newark, DE 19716, USA*

[c] *Department of Chemical Engineering, Villanova University, Villanova, PA 19085, USA*

† Electronic supplementary information (ESI) available. See DOI: 10.1039/c4cy00563e

‡ Address: Department of Chemical and Biomolecular Engineering, University of Pennsylvania, 311A Towne Building, 220 S. 33rd Street, Philadelphia, PA 19104, USA.

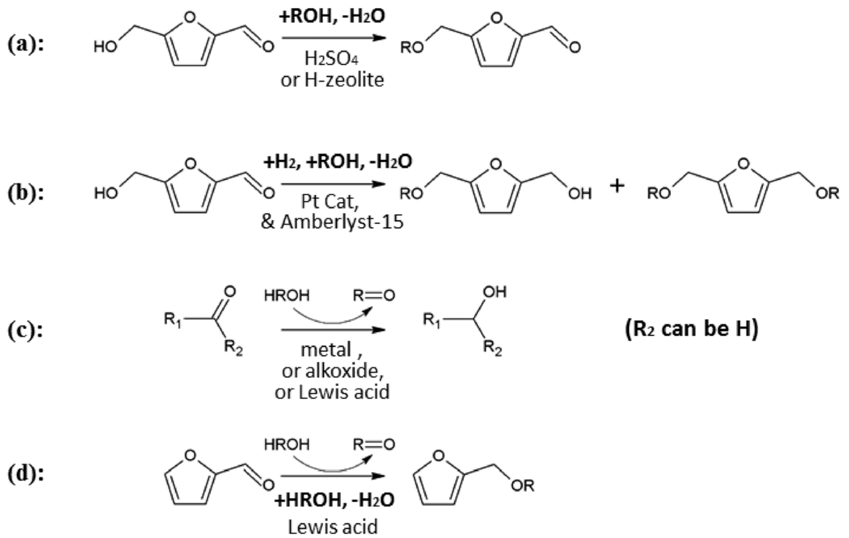

Scheme 1 (a) Direct etherification of HMF, (b) one-pot reductive etherification of HMF *via* hydrogenation, (c) transfer hydrogenation *via* Meerwein–Ponndorf–Verley reaction, and (d) reductive etherification of HMF *via* transfer hydrogenation.

catalyzed by solid, inexpensive oxides. For example, Dumesic and coworkers[12] showed that ZrO_2 can be effective for transfer hydrogenation of levulinic acid/ethyl levulinate to γ-valerolactone. Similarly, Corma *et al.*[13] reported the reduction of cyclohexanone to cyclohexanol in large-pore zeolites with framework Sn or Zr. Presumably, the oxides in these examples are acting as solid Lewis acids. An additional benefit of using solid acids to catalyze transfer hydrogenation is that the acids may also catalyze the etherification reactions. The feasibility of this has been demonstrated by Bui *et al.*[14] and Jae *et al.*,[15] who performed the sequential transfer hydrogenation and etherification of furfural to furfuryl ether over zeolite BEA with framework Zr, Sn and Ti, using an alcohol as hydrogen donor. This reaction is shown in Scheme 1(d).

In the present study, we compare the performance of a range of solid acids for the reaction of HMF with 2-propanol in the liquid phase in order to gain insights into what properties are most desirable for carrying out transfer hydrogenation and the subsequent etherification reactions. We examined both solid Lewis acids (Al_2O_3, ZrO_2, TiO_2, and Sn-BEA) and solid Brønsted acids (H-BEA, Al_2O_3/SBA-15, and ZrO_2/SBA-15). What we will show is that each of the materials showed activity but that the product selectivities varied strongly with the oxide properties (Scheme 2).

Experimental

Materials

A list of the materials used in this study is given in Table 1. The γ-Al_2O_3 (99%, Alfa Aesar) was pre-treated with 1 mol L^{-1} NH_4NO_3 solution in order to remove Na impurities.[16] In the NH_4NO_3 treatment, 500 mg of γ-Al_2O_3 was stirred with 300 mL

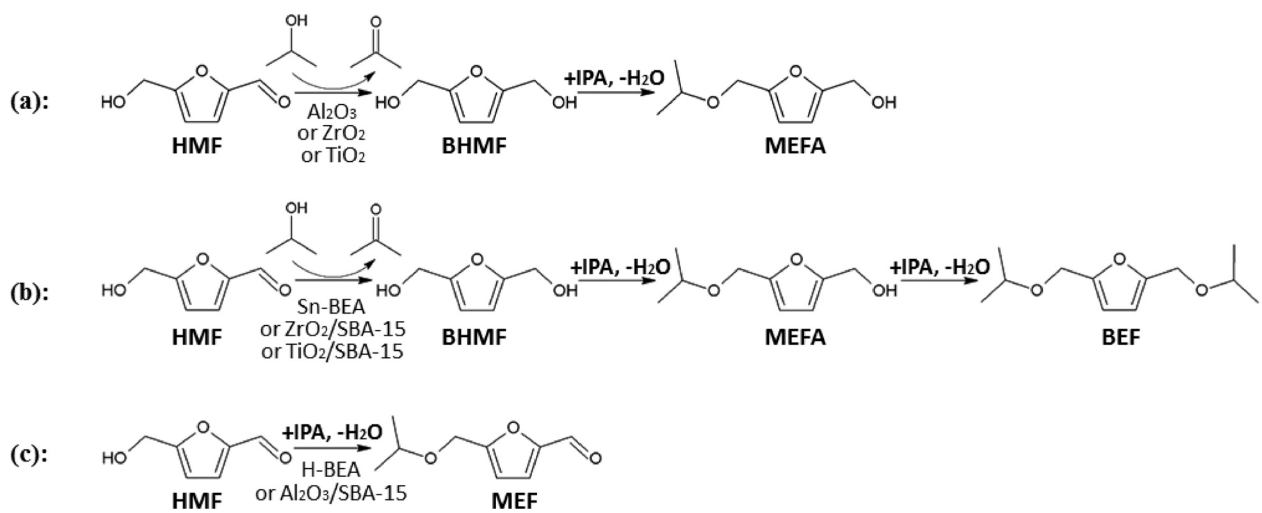

Scheme 2 Reaction schemes of HMF etherification with isopropanol over solid acid catalysts. Compounds: 5-(hydroxymethyl)furfural (HMF), 2,5-bis(hydroxymethyl)furan (BHMF), 5-[(1-methylethoxy) methyl]furfural (MEF), 5-[(1-methylethoxy)methyl]-2-furanmethanol (MEFA), 2,5-bis[(1-methylethoxy)methyl]furan (BEF).

of the solution at 353 K for 3 hours, then calcined to 773 K. The TiO_2 was purchased from Aeroxide (99%) and used without additional pretreatment. The ZrO_2 sample was prepared by drying an aqueous solution of zirconyl nitrate hydrate (99%, Aldrich), followed by calcination at 773 K for 4 h. The H-BEA (zeolite beta, CP811-300), with Si/Al_2 of 200, was obtained from PQ Corporation.

The Sn-BEA, with Si/Sn ratio of 118, was prepared by the procedure described by Corma *et al.*;[13] characterization of this material has been described elsewhere.[15,17] First, 13.6 g of TEOS (Sigma Aldrich, 98%) were hydrolyzed in 13.01 g of TEAOH (40 wt%, Sigma Aldrich) with stirring at room temperature. To this solution, 0.1840 g of $SnCl_4{\cdot}5H_2O$ (Strem Chemicals, 98% reagent grade) in 0.92 g of DI water were added, after which the mixture was again stirred at room temperature until the solution had decreased in weight by 12 g because of ethanol evaporation. To the resulting clear solution, 1.47 g of HF (48 wt%) were added, causing the formation of a thick paste. Next, 0.152 g of calcined, siliceous zeolite Si-Beta in 0.73 g of DI water was added as seed crystals. The final gel composition was as follows: 1.0 SiO_2 : 0.0083 SnO_2 : 0.54 TEAOH : 7.5 H_2O : 0.54 HF. The crystallization was carried out in rotating, Teflon-lined, stainless-steel autoclaves at 413 K for 28 days. The solid produced by this process was then calcined in air using a heating ramp of 3 K min^{-1} to 853 K and held at this temperature for an additional 3 h.

SBA-15-supported Al_2O_3, ZrO_2, and TiO_2 were also prepared and tested. The SBA-15 was a mesoporous silica, with 5.0 nm, uniform, mono-dimensional channels and has been described elsewhere.[18] Al_2O_3/SBA-15 was synthesized to have 10 wt% Al_2O_3 by mixing 1.46 g aluminum nitrate nonahydrate (98.0% to 102.0%, Alfa Aesar) with 1.8 g SBA-15 in 100 mL of water for 2 h at 353 K, followed by evaporation of the water and calcination of the solid at 773 K. The 10 wt% ZrO_2/SBA-15 sample was prepared in the same manner, with a zirconia nitrate aqueous solution (99%, Aldrich). For the 10 wt% TiO_2/SBA-15 sample, 1.8 g SBA-15 powder was stirred with 0.88 mL titanium iso-propoxide (97%, Aldrich) in 100 mL tetrahydrofuran under a N_2 atmosphere. After removing the solvent by evaporation, the solid was again calcined at 773 K for 4 h.

Characterization methods

The surface areas of the samples were determined from N_2 isotherms using Brunauer–Emmett–Teller (BET) method at 78 K, after evacuation of the sample at 500 K, and are reported in Table 1, rounded to the nearest 10 m^2 g^{-1}. Each of the samples was also examined in simultaneous Temperature-Programmed Desorption/Thermogravimetric Analysis (TPD-TGA) measurements. The TPD-TGA experiments were performed by exposing the samples to a few torr of the adsorbate of interest, followed by evacuation to ~10^{-6} torr for 1 h. The sample temperature was then ramped at 10 K min^{-1} while monitoring the sample weights and the partial pressures using a quadrupole mass spectrometer. TPD-TGA of 2-propanamine allows determination of the Brønsted-acid site concentration from the amount of the amine that reacts *via* the Hofmann elimination to form propene and NH_3 between 573 and 650 K.[19] Total acid-site concentrations (Lewis and/or Brønsted) were determined from TPD-TGA of 1-propanol. Although adsorbed 1-propanol will react to propene and water on both Lewis- and Brønsted-acid sites, the temperature at which reaction occurs varies with the nature of the sites.

The reactions of HMF with 2-propanol were carried out in a high-pressure, flow reactor that has been described in detail elsewhere.[20] The tubular reactor was a 20 cm long, stainless-steel tube with a 4 mm ID and 1/4 inch OD, passed through a tube furnace. The liquid feed, a mixture of 1 g HMF (99%, Sigma-Aldrich) and 100 mL isopropanol (99.9%, Fisher Scientific), was introduced into the reactor using an HPLC pump (Series I+, Scientific Systems Inc.) with a fixed feed rate at 0.2 mL min^{-1}. For these measurements, the reactor pressure was maintained at 69 bar using a back-pressure regulator (KPB series, Swagelok). Product analysis was carried out by means of a GC-Mass Spectrometer (QP-5000, Shimadzu), equipped with a capillary column (HP-Innowax, Agilent Technologies). The HMF quantification was achieved by GC/MS using standard solutions with different concentrations. Due to the lack of commercial standards for ethers, the GC sensitivity for the products was assumed to be equal to that for HMF. Due to the uncertainties in the calibration factors, the

Table 1 Site densities and BET surface area of the catalyst samples used in this study

	TPD/TGA of 1-propanol (μmol g^{-1})	TPD/TGA of 2-propanamine (μmol g^{-1})	Site density for TOF calculation (μmol g^{-1})	BET surface area (m^2 g^{-1})
Al_2O_3	200	0	200	150
ZrO_2	120	0	120	40
TiO_2	150	0	150	50
10 wt% Al_2O_3/SBA-15	360	200	360	480
10 wt% ZrO_2/SBA-15	200	130	200	560
10 wt% TiO_2/SBA-15	260	30	260	480
SBA-15	0	0	—	650
H-BEA	—	100	100	—
Sn-BEA	—	0	100[a]	—

[a] The active site density of Sn-BEA was obtained from TPD-TGA measurement adsorbing acetonitrile.

total GC area for all products was used to normalize product selectivities.

To avoid large pressure drops in the reactor, the catalyst samples were first pressed into thin wafers, which were then broken into small pieces before placing them into the reactor. The rectangular wafers had a characteristic size of 1–2 mm and a thickness of approximately 0.3 mm. The catalyst was loosely packed in the reactor, so that the length of the bed was approximately 1 cm for a 0.1 g loading, and 4 cm for a 0.4 g loading. Based on the volumetric flow rate, the linear velocity of the liquid feed was determined to be 1.6 cm min^{-1}. For differential conversions, it was possible to calculate rates from the measured conversions, although characteristic diffusion times (δ^2/D ~ (0.015 cm)^2/10^{-6} cm^2 s^{-1} ~ 200 s) could affect this somewhat. However, channeling of the reaction fluid around the catalyst particles prevents measurement of rates at higher conversions. In this study, catalyst loading was varied in order to determine the effect of increasing conversion on the selectivity and cannot be used as a measure of reaction rates.

To determine the effect of temperature, reactions were carried out with 0.1 g of catalyst at 413 K and 453 K. (For the H-BEA and Sn-BEA catalysts, reactions were also measured with 0.05 g at 413 K in order to maintain differential conversions.) The conversions were negligible in the absence of a catalyst and also with unmodified SBA-15. For each of the catalysts examined in this study, conversions and selectivities remained unchanged over the period of several hours required to make the measurements. The typical run time was 3 h, and the outlet products were sampled every 30 min. In all cases, minimal changes were observed in the conversion and selectivity; and representative data was typically chosen from the second or third measurement (40 to 60 min after starting the reaction).

Results and discussion

Catalyst characterization

A summary of the most important properties for each of the materials used in this study is given in Table 1 and the methods used to obtain those values will be described here. Brønsted-acid site concentrations were determined from TPD-TGA results following room-temperature adsorption of 2-propanamine, as shown in Fig. 1, which were measured on the Al_2O_3/SBA-15 sample. On γ-Al_2O_3, it has previously been reported that all of the amine desorbs intact over a broad temperature range, from room temperature to 700 K.[16] The high desorption temperature demonstrates that adsorption is strong but the fact that there is no reaction implies a complete absence of Brønsted-acid sites. This result is in sharp contrast to that found for the Al_2O_3/SBA-15 sample. Following exposure to the amine and evacuation, approximately 200 μmol g^{-1} of the amine reacts to propene and ammonia between 575 and 650 K. Although the Brønsted-site concentration on Al_2O_3/SBA-15 is significantly lower than the Al concentration (~2000 μmol g^{-1}), it is much higher than is normally found on amorphous silica–alumina catalysts.[21,22] We suggest that the amorphous silica walls making up the SBA-15 are exceptionally capable of incorporating Al^{3+} into tetrahedral positions in the siliceous matrix.

The TPD-TGA results for 2-propanamine on pure and SBA-15-supported ZrO_2 and TiO_2 were unexpectedly similar to that found for Al_2O_3. Again, the pure oxides showed no Brønsted acidity, while the SBA-15-supported oxides both showed significant concentrations of Brønsted-acid sites, 130 μmol g^{-1} for ZrO_2/SBA-15 and 30 μmol g^{-1} for TiO_2/SBA-15, as determined by the reaction of the amine between 575 and 650 K. Evidence for Brønsted acidity in some zirconia silicates has been presented previously, based on isomerization of butane

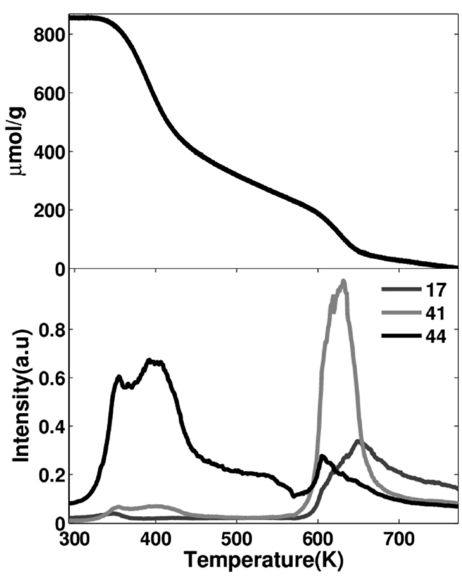

Fig. 1 TPD-TGA curves for 2-propanamine over 10 wt% Al_2O_3/SBA-15.

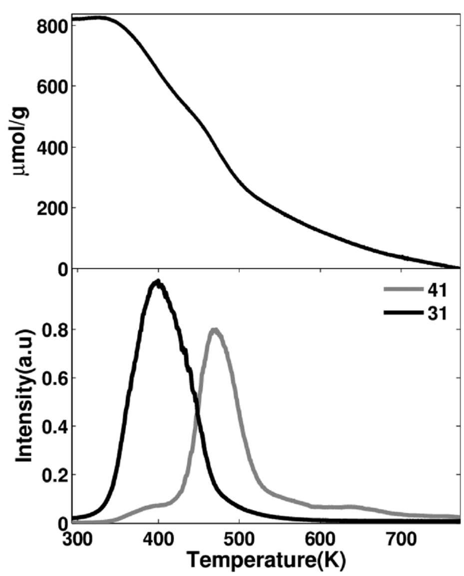

Fig. 2 TPD-TGA curves for 1-propanol over 10 wt% Al_2O_3/SBA-15.

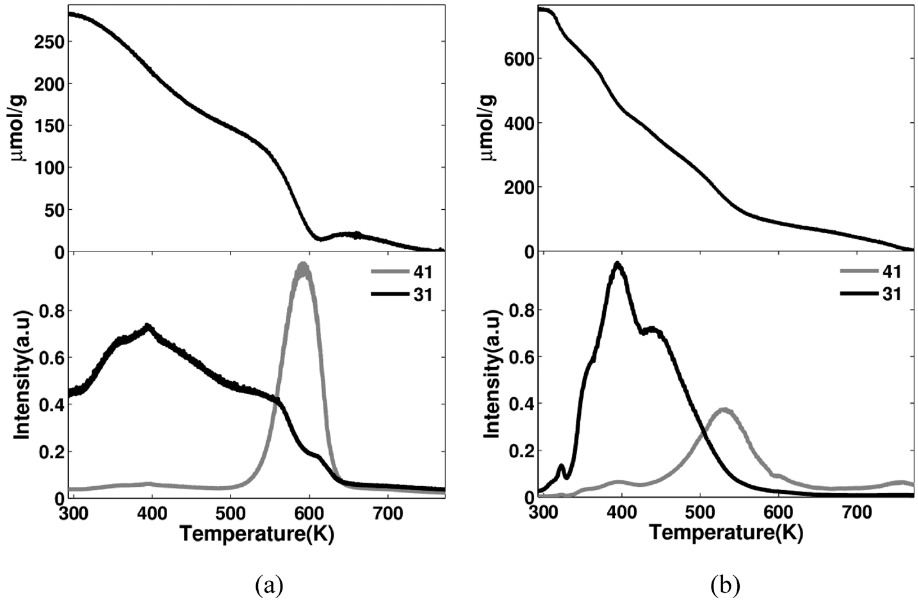

Fig. 3 TPD-TGA curves for 1-propanol over (a) ZrO_2, (b) 10 wt% ZrO_2/SBA-15.

and on the formation of pyridinium ions in FTIR measurements.[23] Obviously, the nature of Brønsted-acid sites formed by Zr^{4+} and Ti^{4+} in silica is not expected to be similar to that of sites formed by tetrahedral Al^{3+}.

TPD-TGA measurements of 1-propanol are complementary in that the alcohol reacts on both Lewis- and Brønsted-acid sites. Results for γ-Al_2O_3[15] and an H-ZSM-5 zeolite[24] have been published elsewhere. As with 2-propanamine, some of the adsorbed 1-propanol leaves the sample unreacted. On γ-Al_2O_3, 1-propanol molecules at Lewis-acid sites undergo dehydration over a narrow temperature range centered at approximately 550 K; on H-ZSM-5, molecules associated with the Brønsted sites react at approximately 460 K. TPD-TGA data for Al_2O_3/SBA-15 are shown in Fig. 2 and are qualitatively more similar to the results for H-ZSM-5. Approximately 800 μmol g^{-1} of the alcohol remains on the sample following room-temperature exposure, followed by evacuation for 1 h. During the temperature ramp, 360 μmol g^{-1} of the alcohol react over a broad temperature range centered at 480 K. Because this is close to the reaction temperature observed with Brønsted sites on H-ZSM-5, we suggest that the lower dehydration temperature on Al_2O_3/SBA-15 compared to γ-Al_2O_3 is associated with reaction on Brønsted-acid sites. The increased width of the reaction feature on Al_2O_3/SBA-15 may be due to the presence of a mixture of Brønsted- and Lewis-acid sites, since the concentration of sites able to react 1-propanol was larger than the concentration of Brønsted-acid sites determined by 2-propanamine adsorption.

TPD-TGA curves for the 1-propanol adsorption on ZrO_2 and ZrO_2/SBA-15 are shown in Fig. 3. The acid-site concentrations, as determined by the amount of 1-propanol that dehydrates, were 120 and 200 μmol g^{-1} on these two samples, respectively. The peak temperature for propene formation on pure ZrO_2 was 590 K, which is approximately 40 K higher than with γ-Al_2O_3, implying that the Lewis-acid sites on ZrO_2 are somewhat weaker. Because the concentration of sites able to dehydrate 1-propanol on ZrO_2/SBA-15 was similar to the Brønsted-acid site concentration, most of the 1-propanol

Table 2 Turnover rates and product selectivities of HMF etherification with IPA at 413 K[a]

Catalyst	Conv. (%)	TOF (10^{-3} molec per site s^{-1})	Product selectivity (%)			
			MEF	BHMF	MEFA	BEF
Al_2O_3	11.1	1.45	—	55.4	44.7	—
ZrO_2	7.1	1.56	—	91.0	9.0	—
TiO_2	3.7	0.65	—	79.4	20.6	—
10 wt% ZrO_2/SBA-15	12.1	1.60	—	—	31.4	68.6
10 wt% TiO_2/SBA-15	6.9	0.70	31.7	—	20.5	47.9
Sn-BEA	12.8	6.71	9.8	—	7.4	82.5
10 wt% Al_2O_3/SBA-15	11.4	0.83	91.5	—	—	8.5
H-BEA	14.6	7.20	97.9	—	—	2.1

[a] MEF: mono-ether furfural, 5-[(1-methylethoxy)methyl]furfural; MEFA: mono-ether furfuryl alcohol, 5-[(1-methylethoxy)methyl]-2-furanmethanol; BEF: bis-ether furan, 2,5-bis[(1-methylethoxy)methyl]furan; BHMF: 2,5-bis(hydroxymethyl)furan.

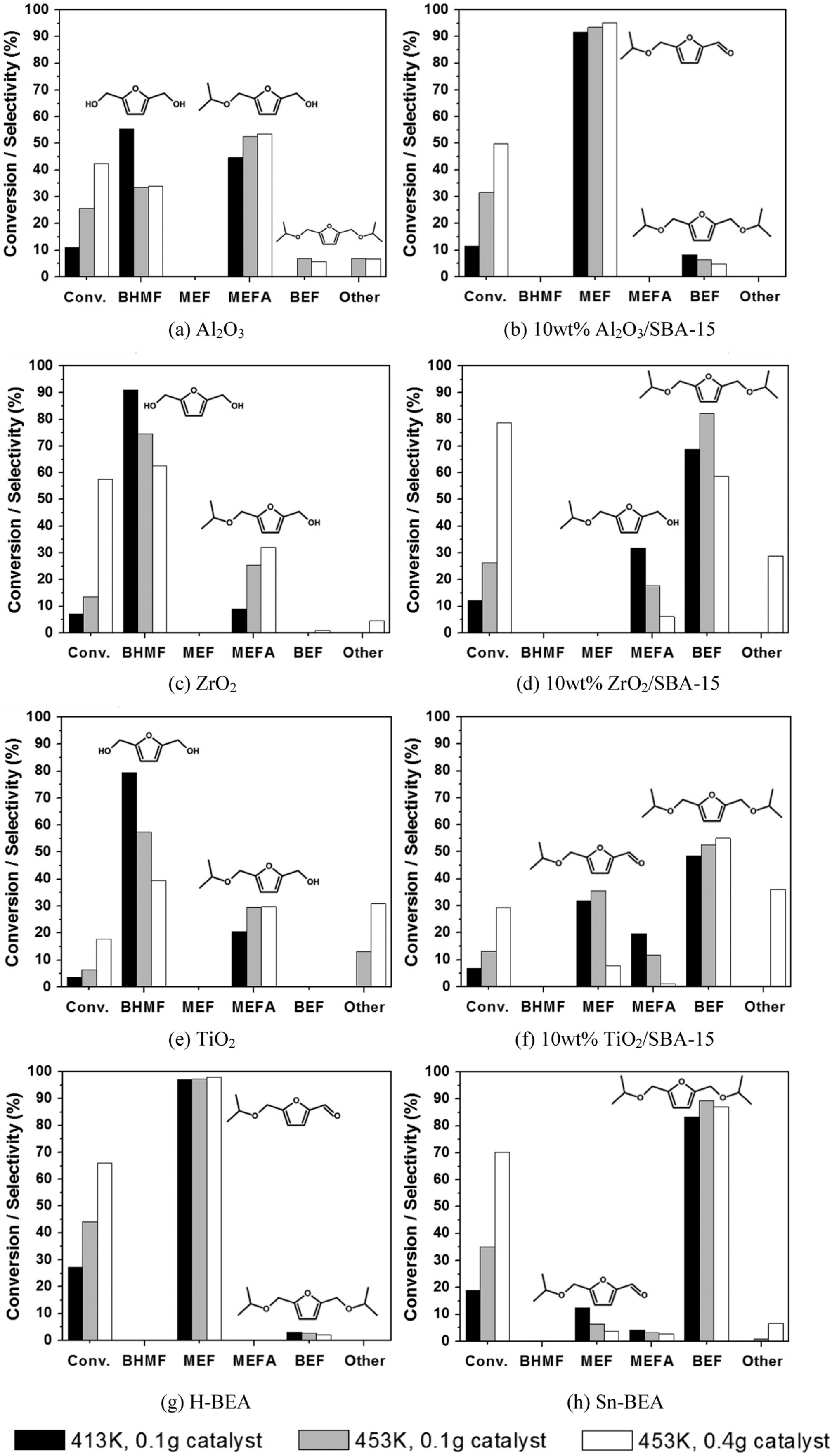

Fig. 4 HMF conversion and product distributions over different catalysts as a function of temperature and catalyst loading.

reacting on this sample are likely associated with Brønsted sites, which may explain the lower reaction temperature on this sample, ~540 K. Previously, changes in the peak temperature for dehydration of alcohols at Brønsted sites associated with framework Fe or Al in siliceous zeolites has been shown to correlate with the activity of those sites.[25] Therefore, using the dehydration temperature as a measure of site strength, the Brønsted sites in ZrO_2/SBA-15 must be significantly weaker than those in Al_2O_3/SBA-15.

Results for adsorption of 1-propanol on TiO_2 and TiO_2/SBA-15 are not shown because they were similar to that obtained with ZrO_2 and ZrO_2/SBA-15. The site density as determined by the amount of 1-propanol that reacted was slightly higher on TiO_2 compared to ZrO_2, 150 μmol g^{-1} *versus* 120 μmol g^{-1}; but the dehydration temperatures were identical within experimental error. The SBA-15 support had less effect on the dehydration peak temperature with TiO_2 (The dehydration peak temperature on TiO_2/SBA-15 was 620 K.), which is likely due to the fact that the Brønsted site concentration was much lower on TiO_2/SBA-15 that on ZrO_2/SBA-15.

Reaction studies

The liquid-phase reaction (69 bar) of HMF with 2-propanol (1 g HMF dissolved in 100 mL of 2-propanol) on each of the catalysts was characterized using a fixed feed rate of 0.2 mL min^{-1}. The measurements were carried out with 0.1 g of each catalyst at 413 and 453 K to determine the effect of temperature on conversion and selectivity and with 0.4 g of each catalyst at 453 K to determine how selectivity changed with conversion at this temperature. All of the catalysts were stable over the period of several hours used in making the measurements and no conversion was observed in the absence of a catalyst. While we have focused on the products formed from HMF, we also observed formation of acetone from the 2-propanol in amounts equal to that required for the transfer hydrogenation rates. The data at 413 K emphasizes the initial products formed at low conversions and is shown in Table 2. (Note: the data in Table 2 for H-BEA and Sn-BEA were determined using a catalyst loading of 0.05 g in order to maintain the conversion below 10%.) All of the reaction results are summarized in graphical form in Fig. 4.

Since the conversions in Table 2 were all less the 10%, these data appear to represent the initial products that are formed in the reaction. Several clear trends appear. H-BEA and Al_2O_3/SBA-15 have strong Brønsted-acid sites and are both highly selective for MEF. As expected based on literature reports, these catalysts are highly active for ether formation but less active for transfer hydrogenation. By contrast, the pure oxides, which exhibit purely Lewis acidity, are much more active for transfer hydrogenation reactions. On ZrO_2, the selectivity for the di-alcohol, 2,5-bis(hydroxymethyl)furan (BHMF), was over 90%. BHMF can go on to form the mono-ether alcohol, 5-[(1-methylethoxy)methyl]-2-furanmethanol (MEFA), and the di-ether, 2,5-bis[(1-methylethoxy)methyl]furan (BEF), on the more acidic oxides. The Lewis-acid sites on Sn-BEA were the most active, showing a high selectivity to 2,5-bis[(1-methylethoxy)methyl]furan (BEF) even at low total conversions. Interestingly, ZrO_2 and TiO_2 on SBA-15 were also quite selective towards formation of BEF, presumably by carrying the MPV interhydride transfer from 2-propanol to the carbonyl of HMF on the Lewis acid sites followed by etherification on the Brønsted acid sites of the catalyst.

Turnover frequencies, based on HMF consumption, were estimated for each of the catalysts using site densities calculated from the amount of 1-propanol that reacted in TPD-TGA measurements. The only obvious trend is that both H-BEA and Sn-BEA were much more active than either the pure oxides or the oxides supported on SBA-15. This might suggest that the zeolite cavities have a confining effect that increases the reaction rates. Alternatively, change in coordination of the metal atom may also play a role in the observed turnover frequencies.

As shown in Fig. 4, increasing the temperature to 453 K did not change the overall picture. As expected, the conversions increased and selectivities for MEFA and BEF increased at the expense of BHMF formation on those catalysts that are active for transfer hydrogenation. Similarly, increasing the catalyst loading did not significantly alter the conclusions, other than to suggest that MEFA and BEF can undergo additional reactions to form unidentified side products. This was especially noticeable with ZrO_2/SBA-15. Interestingly, MEF does not seem to undergo additional reactions on H-BEA or Al_2O_3/SBA-15, since the selectivity for MEF remained high at the higher conversions. Once MEF is formed, further reaction to the desired product, BEF, does not occur.

Overall, the results from this study show surprisingly simple product distributions for the reaction of HMF with 2-propanol over a variety of solid catalysts, although the selectivities were remarkably different depending on the nature of the oxide. Lewis acidity appears to be essential for transfer hydrogenation, since the reaction was almost completely absent on H-BEA and Al_2O_3/SBA-15, which are primarily Brønsted acids. These strong Brønsted acids produce the mono-ether (MEF), which appears to be resistant to transfer hydrogenation. Bulk ZrO_2 and TiO_2, which are Lewis acids only, were both reasonably active for hydrogen transfer but less active for the etherification reactions. The weak Brønsted acidity that was added by supporting these oxides on SBA-15 enhanced that activity substantially; however, Brønsted acidity is clearly not required for etherification, given that Sn-BEA was very active and selective for production of the di-ether.

One very interesting question arising from this work involves how to characterize Lewis acidity and then relate it to catalytic activity. A previous adsorption study with alcohols on Sn-BEA showed that *tert*-butanol adsorbed at Sn sites started to undergo dehydration beginning at ~370 K in TPD-TGA.[17] By comparison, the same dehydration reaction on γ-Al_2O_3 commenced above 400 K.[16] On the other hand, diethyl ether, which is expected to have a similar reactivity to ethanol or 1-propanol given that reaction involves a primary carbenium ion, desorbed from the Sn sites unreacted, while γ-Al_2O_3 was able to promote dehydration prior to desorption. The difference here may be simply due to the ability of on γ-Al_2O_3 to hold the alcohols to high temperatures, which does not itself seem to be a good measure of acid strength.

Finally, it is worth noting that the chemistries observed in this study were all possible without having a precious metal or gaseous hydrogen. There was also no attempt to optimize the materials used in this study; the addition of dopants to modify the acidic properties could well lead to improved selectivities. This is still a relatively new avenue for research.

Conclusion

The liquid-phase reaction of HMF with 2-propanol can be catalyzed by a wide range of oxide catalysts. γ-Al_2O_3, ZrO_2, and TiO_2 are all Lewis acids that are able to carry out transfer hydrogenation of the aldehyde functionality in HMF, as well as form a mono-ether. Strong Bronsted sites, present in H-BEA and Al_2O_3/SBA-15, catalyze formation of a mono-ether without hydrogenation of the carbonyl. Weak Brønsted sites are formed when ZrO_2 and TiO_2 are supported on SBA-15 and these promote ether formation following transfer hydrogenation. Sn-BEA, which contains only Lewis acid sites, was the most active catalyst for transfer hydrogenation and ether formation.

Acknowledgements

We acknowledge support from the Catalysis Center for Energy Innovation, an Energy Frontier Research Center funded by the U.S. Department of Energy, Office of Science, Office of Basic Energy Sciences under award no. DE-SC0001004.

References

1 M. Balakrishnan, E. R. Sacia and A. T. Bell, *Green Chem.*, 2012, **14**, 1626–1634.
2 G. W. Huber, J. N. Chheda, C. J. Barrett and J. A. Dumesic, *Science*, 2005, **308**, 1446–1450.
3 R. E. O'Neill, L. Vanoye, C. D. Bellefon and F. Aiouache, *Appl. Catal., B*, 2014, **144**, 46–56.
4 J. N. Chheda and J. A. Dumesic, *Catal. Today*, 2007, **123**, 59–70.
5 E. Salminen, N. Kumar, P. Virtanen, M. Tenho, P. Maki-Arvela and J. P. Mikkola, *Top. Catal.*, 2013, **56**, 765–769.
6 E. J. Ras, S. Maisuls, P. Haesakkers, G. J. Gruter and G. Rothenberg, *Adv. Synth. Catal.*, 2009, **351**, 3175–3185.
7 E. R. Sacia, M. Balakrishnan and A. T. Bell, *J. Catal.*, 2014, **313**, 70–79.
8 A. Rahman and S. S-Al-Deyab, *Appl. Catal., A*, 2014, **469**, 517–523.
9 D. G. I. Petra, J. N. H. Reek, P. C. J. Kamer, H. E. Schoemaker and P. W. N. M. van Leeuwen, *Chem. Commun.*, 2000, 683–684.
10 A. Mollica, S. Genovese, F. Pinnen, A. Stefanucci, M. Curini and F. Epifano, *Tetrahedron Lett.*, 2012, **7**, 890–892.
11 S. N. Misra, R. S. Shukla and M. A. J. Gagnani, *J. Colloid Interface Sci.*, 2005, **281**, 164–170.
12 M. Chia and J. A. Dumesic, *Chem. Commun.*, 2011, **47**, 12233–12235.
13 A. Corma, M. E. Domine and S. Valencia, *J. Catal.*, 2003, **215**, 294–304.
14 L. Bui, H. Luo, W. R. Gunther and Y. Roman-Leshkov, *Angew. Chem., Int. Ed.*, 2013, **52**, 8022–8025.
15 J. Jae, E. Mahmoud, R. F. Lobo and D. G. Vlachos, *ChemCatChem*, 2014, **6**, 508–513.
16 S. Roy, G. Mpourmpakis, D. Hong, D. G. Vlachos, A. Bhan and R. J. Gorte, *ACS Catal.*, 2012, **2**, 1846–1853.
17 S. Roy, K. Bakhmutsky, E. Mahmoud, R. F. Lobo and R. J. Gorte, *ACS Catal.*, 2013, **3**, 573–580.
18 M. A. Smith, M. G. Ilasi and A. Zoelle, *J. Phys. Chem. C*, 2013, **117**, 17493–17502.
19 R. J. Gorte, *Catal. Lett.*, 1999, **62**, 1–13.
20 J. Luo and R. J. Gorte, *Catal. Lett.*, 2013, **143**, 313–316.
21 J. Tittensor, R. J. Gorte and D. Chapman, *J. Catal.*, 1992, **138**, 714–720.
22 C. Pereira and R. J. Gorte, *Appl. Catal., A*, 1992, **90**, 145–157.
23 J. B. Miller and E. I. Ko, *J. Catal.*, 1996, **159**, 58–68.
24 M. T. Aronson, R. J. Gorte and W. E. Farneth, *J. Catal.*, 1986, **98**, 434–443.
25 T. J. Gricus Kofke, G. T. Kokotailo and R. J. Gorte, *J. Catal.*, 1989, **116**, 252–262.